Semiconductor Optoelectronics
ISSN: 1001-5868

STRUCTURAL AND IR SPECTRAL STUDIES OF MG-SUBSTITUTED LITHIUM FERRITES

Bhoodevi P. Bhandare[1a], Satishkumar Lature[1a#], Rajendra M. Sangshetty[1], Vijay A Hiremath[2], and Ghanshyam H. Jadhav[3]

[1]Dept of Physics, Poojya Doddappa Appa College of Engineering, Kalaburagi-585102, Karnataka, India

[2]Dept of Chemistry, Poojya Doddappa Appa College of Engineering, Kalaburagi-585102, Karnataka, India

[2]Dept. of Physics, Shri Chattrapati Shivaji College, Omerga-416606, Maharashtra, India

[#]Email: satishkumarlature@gmail.com

[a]These authors contributed equally

Abstract

$Li_{0.5-0.5x}Mg_xFe_{2.5-0.5x}O_4$ (x = 0, 0.1, 0.2, 0.3, 0.4, 0.5 and 0.6) mixed spinel ferrites were already prepared using combustion method. The X-ray diffraction spectra of all prepared are taken at room temperature. Using 'POWDER X' software all major peaks of the prepared samples are indexed and confirms the formation of cubic spinel ferrite structure. As Mg-concentration increases in the prepared spinel ferrites the lattice constant also increases obeying Vegard's law. Average crystallite size of all prepared spinel ferrites is found to be in the range 31 - 34 nm. Cation distribution is suggested based on the X-ray data and is confirmed by the lattice parameters a_{th} and a_{exp} are in close agreement with a general trend of increasing as the Mg-concentration is increased. IR spectra of all prepared spinel ferrites show two major bands v_1 and v_2, attributed to stretching vibrations of octahedral and tetrahedral sites of spinel ferrites respectively. Formation of subsidiary bands in all prepared samples confirms the substitution of Mg^{2+} are occupying octahedral and tetrahedral sites of spinel ferrites. Force constant for the tetrahedral and octahedral sites was calculated using IR spectra data. Elastic moduli are calculated and found that the values are decreasing with increase in Mg-concentration. The linear dependence of rigidity modulus with young's modulus suggests the isotropic nature of spinel ferrites. Debye temperature of all prepared ferrites are calculated using Waldron and Anderson model.

Keywords: *Mg-substitutedLithium ferrites, nanoparticles, X-ray spectra, FTIR, Elastic moduli. Debye temperature.*

1. Introduction:

Lithium ferrites and mixed-lithium ferrites have been studied extensively because of their squareness of the hysteresis loop with superior high-temperature performance made it prime candidate for microwave device applications [1-4]. Electrical and magnetic properties of mixed lithium ferrites were greatly dependence on substitution types and reported [5,6]. As nano crystalline lithium ferrites exhibit enhanced structural, electrical and magnetic properties compared to their bulk ferrites and hence desirable for magnetic storage and many more such

applications [7-10].

Due to irreversible loss of lithium and oxygen during the sintering in conventional high temperature ceramic method has restricted the application of mixed lithium ferrites. Compared to conventional ceramic method which involves high temperature (>1000ºC) the coprecipitation [11], hydrothermal [12], micro-emulsion [13], sol-gel method [14], auto combustion [15] are the alternate methods to prepare mixed lithium ferrites at reduced temperatures. Therefore, auto combustion method provides an easy alternative method for preparation of nano crystalline mixed lithium ferrites. However, there are few reports on magnesium substituted lithium ferrites [16-18].

The present work reports the systematic study of Mg-substituted Lithium ferrites by structural investigation such as X-ray diffraction and IR spectrawhich are already prepared by auto combustion method using PEG as fuel [19].

2. Materials and methods:

Mg-substituted Lithium ferrites with the general composition formula $Li_{(0.5-0.5x)}Mg_xFe_{(2.5-0.5x)}O_4$ (where x = 0,0.1,0.2,0.3,0.4&0.5) were prepared by combustion method using PEG as fuel at 450ºC. The details of the procedure used for the synthesis of the sample is described elsewhere[19]. To confirm the formation spinel structure X-ray spectra of all the prepared samples are taken by Philips PW 1051 diffractometer using Cu K_α radiation source. Data collection is done in the range20º to 80º in 2θ. With the processing parameters set in 'POWDER X' software such as: cubic- crystal system, F-type lattice, Cu- radiation, λ – 1.54178Å and ±0.05º - an error for 2θ. The IR spectra are recorded on Perkin-Elmer FTIR spectrometer in the range 300 to 800 cm^{-1} in the KBr medium.

3. Results and Discussion

3.1 X-ray diffraction spectra of spinel ferrites

X-ray diffraction spectra of magnesium substituted Li-ferrites with general formula $Li_{0.5-0.5x}Mg_xFe_{2.5-0.5x}O_4$ (x=0,0.1,0.2,0.3,0.4 and 0.5) are shown in figure(1).Using the software 'POWDER X' all major peaks are indexed and reflection plane (220), (311), (400), (422), (511) and (440) confirming the formation of cubic spinel structure.

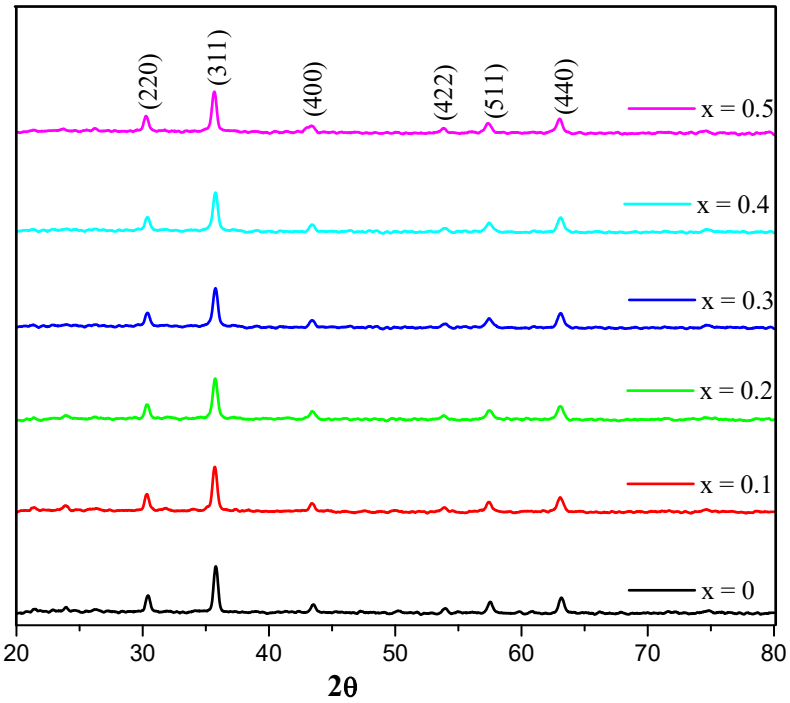

Fig. 1: X-ray spectra of diffraction pattern of $Li_{0.5-0.5x}Mg_xFe_{2.5-0.5x}O_4$ ferrites.

The experimental lattice parameter (a_{exp}) is calculated using the relation,

$$a_{exp} = \frac{dhkl}{\sqrt{h^2+k^2+l^2}} \text{-------(1)}$$

Addition of Mg^{2+}ions into lithium ferrites cause to a small shift of peaks towards lower 2θ values. This shift in peaks shows a change in lattice constant. Using the same software lattice constant of all the prepared samples are calculated and tabulated in table (1), are in close agreement with the reported value [16]. The variation of lattice constant with Mg-concentration is shown in figure (2) which reveals that the lattice constant increases with increasing magnesium concentration and obeys Vegard's law. This is due to the fact that the larger ionic radius ofMg^{2+}(0.78Å) replacing smaller ionic radius cations such as Fe^{3+} (0.64Å) and Li^{+} (0.73Å) and will induce uniform strain in the lattice as the complex is elastically deformed [16, 20].

Average crystallite sizeis estimated using the Debye–Scherrer relation

$$D = \frac{0.9\lambda}{\beta \cos\theta} \quad \text{--------(2)}$$

where λiswavelength of x-ray, $\beta$is full width at half maximum and θ is Bragg's diffraction angle. Particle size of the sample are observed to be in the range between 31-34 nm. The X-ray density is calculated using the relation,

$$\rho_x = \frac{8M}{Na^3} \text{----------(3)}$$

where N is the Avogadro number, M is molecular weight and a is lattice constant. The observed values of X-ray density are in the range between 4.64-4.78 gm/cc and are summarized in table (1).

Table 1: Lattice constant, crystallite size and X-ray density of $Li_{0.5-0.5x}\ Mg_x\ Fe_{2.5-0.5x}\ O_4$.

Mg – Concentration	Lattice constant a_{exp} (nm)	Crystallite size (nm)	x-ray density (gm/cc)	Lattice constant a_{th} (nm)	Ionic Radii (nm)		Bond Length (nm)	
					r_A	r_B	(A – O)	(B – O)
x = 0	0.8316	32.48	4.78	0.8312	0.0685	0.0734	0.1944	0.1995
x = 0.1	0.8338	31.24	4.73	0.8333	0.0690	0.0739	0.1950	0.1999
x = 0.2	0.8341	33.15	4.71	0.8340	0.0693	0.0740	0.1953	0.2000
x = 0.3	0.8343	34.17	4.69	0.8342	0.0693	0.0741	0.1954	0.2000
x = 0.4	0.8346	32.25	4.67	0.8345	0.0695	0.0741	0.1956	0.2000
x = 0.5	0.8349	33.22	4.65	0.8348	0.0696	0.0742	0.1956	0.2001

In the present investigation we propose cation distribution of $Li_{0.5-0.5x}\ Mg_x\ Fe_{2.5-0.5x}\ O_4$ferrite by taking into the account that Li-ferrite has inverse spinel structure,has been suggested as expressed in table (2). The validity of the suggested cation distribution can be examined by calculating the theoretical lattice constant using the following relations [16].

Theoretical lattice constant,

$$a_{th}=\frac{8}{3\sqrt{3}}[(r_A+R_0) + \sqrt{3}(r_B+R_0)] \quad \text{----------(4)}$$

Tetrahedral ionic radius,

$$r_A = yr_{Mg}+(1-y)\ r_{FeA} \quad \text{--------(5)}$$

Octahedral ionic radius,

$$r_B = [0.5-(0.5x)]\ r_{Li} + (x-y)\ r_{Mg} +[1.5-0.5(x+y)]\ r_{FeB} \text{-------(6)}$$

where r_{mg} , r_{FeA}, r_{FeB} and r_{Li} are the ionic radii of magnesium, ferric (A & B site) and Lithium ions respectively.

Bond lengths of T_h (A – O) and O_h (B – O) sites are calculated using the following equations [21].

$$A - O =\left(\mu - \frac{1}{4}\right) a\sqrt{3} \text{ -------(7)}$$

$$B - O = \left(\frac{5}{8} - \mu\right) a \text{ ----------(8)}$$

where μ is the oxygen ion parameter given by

$$\mu = \left(\frac{r_A+R_0}{a\sqrt{3}}\right) + 0.25 \text{ ------(9)}$$

where, R_0 = 0.126 nm (oxygen ion radius)

The calculated values of ionic radii and bond lengths are presented in table (2). The variation of lattice constant with Mg- concentration is shown in figure (2). It is noticed that ionic radii r_A and r_B and bond lengths (A – O) & (B – O) slightly increase with increase in Mg^{2+}

content. This is attributed to large ionic Mg^{2+} ions replace Fe^{3+} ions occupy B-site and partially occupy A- site, this is good agreement with previously suggested cation occupancy by Baijal [16] and Widatallah [17]. Table (2) shows both values of the lattice parameters a_{th} and $a_{exp}$are in close agreement with a general trend of increasing as the Mg-concentration is increased which confirm the validity of the suggested cation distribution.

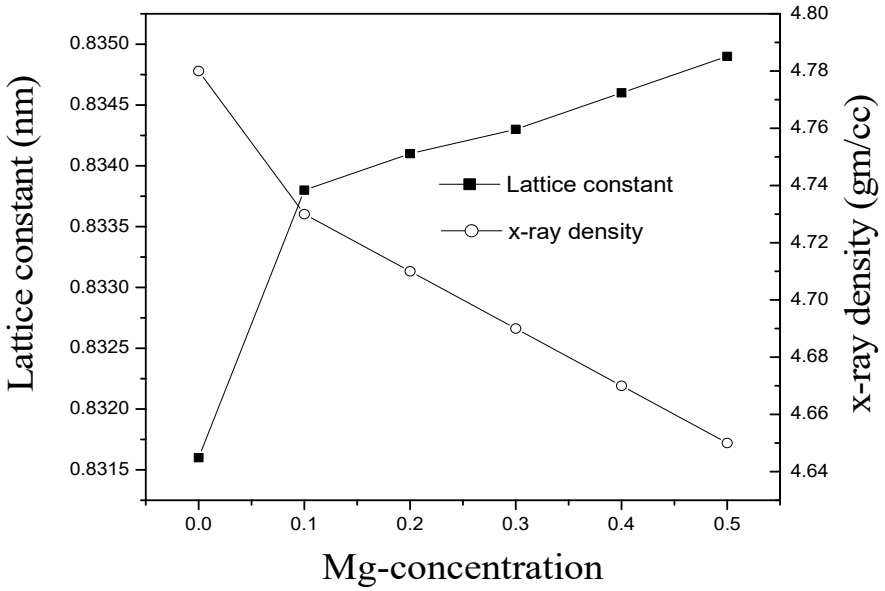

Fig 2: Variation of Mg-concentration with lattice constant and x-ray density

As the intensity ratios of the planes $I_{(hkl)}/I_{(400)}$ and $I_{(hkl)}/I_{(422)}$ are sensitive to the cation distribution [22, 23].Using the X-ray data of all prepared samples the intensity ratios $I_{(220)}/I_{(400)}$, $I_{(311)}/I_{(400)}$,$I_{(511)}/I_{(400)}$,$I_{(440)}/I_{(400)}$are calculated and plotted against Mg-concentration as shown in figure (3a). As Mg-concentration increases the ratio $I_{(hkl)}/I_{(400)}$decreases, attributed to the migration of Fe^{3+} from tetrahedral to octahedral sites which is confirmed with decrease in the ratio $(Fe^{3+})_A/[Fe^{3+}]_B$. The ratio $(Fe^{3+})_A/[Fe^{3+}]_B$ is calculated and plotted against Mg-concentration as shown in figure (3b).

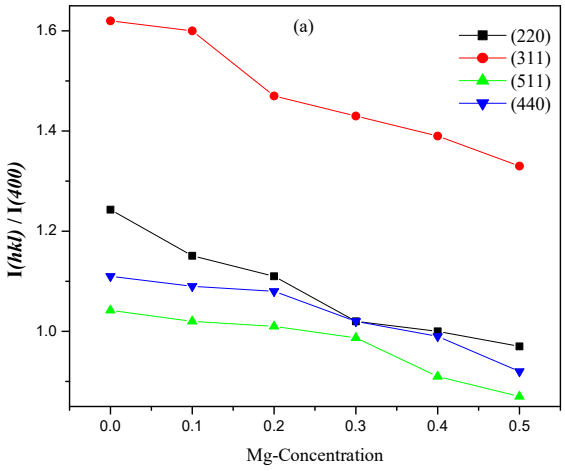

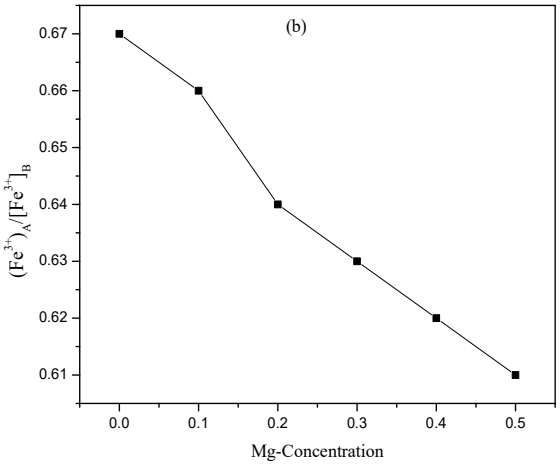

Fig 3:(a) The intensity ratios of I*(hkl)*/I*(400)* with Mg-concentration**(b)** The ratio of Fe^{3+}ions on tetrahedral and octahedral sites of Mg-substituted Lithium ferrites.

Table 2: Cation distribution of $Li_{0.5-0.5x}\ Mg_x\ Fe_{2.5-0.5x}\ O_4$

Mg – Concentration	**Chemical Composition**	**Cation distribution**	**$I_{(422)}/I_{(440)}$**	**$[Mg^{2+}]_B/(Mg^{2+})_A$**
x = 0	$Li_{0.5}Fe_{2.5}O_4$	$(Fe)[Li_{0.5}Fe_{1.5}]O_4$	2.75	2.33
x = 0.1	$Li_{0.45}Mg_{0.1}Fe_{2.45}O_4$	$(Mg_{0.03}Fe_{0.97})[Li_{0.45}Mg_{0.07}Fe_{1.48}]O_4$	2.65	2.33
x = 0.2	$Li_{0.4}Mg_{0.2}Fe_{2.4}O_4$	$(Mg_{0.06}Fe_{0.94})[Li_{0.4}Mg_{0.14}Fe_{1.46}]O_4$	2.68	2.33
x = 0.3	$Li_{0.35}Mg_{0.3}Fe_{2.35}O_4$	$(Mg_{0.09}Fe_{0.91})[Li_{0.35}Mg_{0.21}Fe_{1.44}]O_4$	2.78	2.33
x = 0.4	$Li_{0.3}Mg_{0.4}Fe_{2.3}O_4$	$(Mg_{0.12}Fe_{0.88})[Li_{0.3}Mg_{0.28}Fe_{1.42}]O_4$	2.68	2.33
x = 0.5	$Li_{0.25}Mg_{0.5}Fe_{2.25}O_4$	$(Mg_{0.15}Fe_{0.85})[Li_{0.25}Mg_{0.35}Fe_{1.4}]O_4$	2.75	2.33

3.2 IR spectra of spinel ferrites:

The IR spectraof $Li_{0.5-0.5x}\ Mg_x\ Fe_{2.5-0.5x}\ O_4$are shown in figure (4), which shows two distinct vibrational bands v_1 and v_2 corresponding to the cations situated in the tetrahedral A-site (Th) and the octahedral B- site (Oh).The band between nearly 300 – 510 cm^{-1} corresponding to v_1 are assigned to the stretching vibrations of O_h complexes and the band between nearly 510 – 750 cm^{-1}corresponding to v_2 assigned to the stretching vibrations of the T_h complexes. The tetrahedral ions vibrate along the line joining the cation andneighboring oxygen ions, while the octahedral cations vibrate in a direction perpendicular to the axis joining the tetrahedral metal ion and oxygen ion [24].

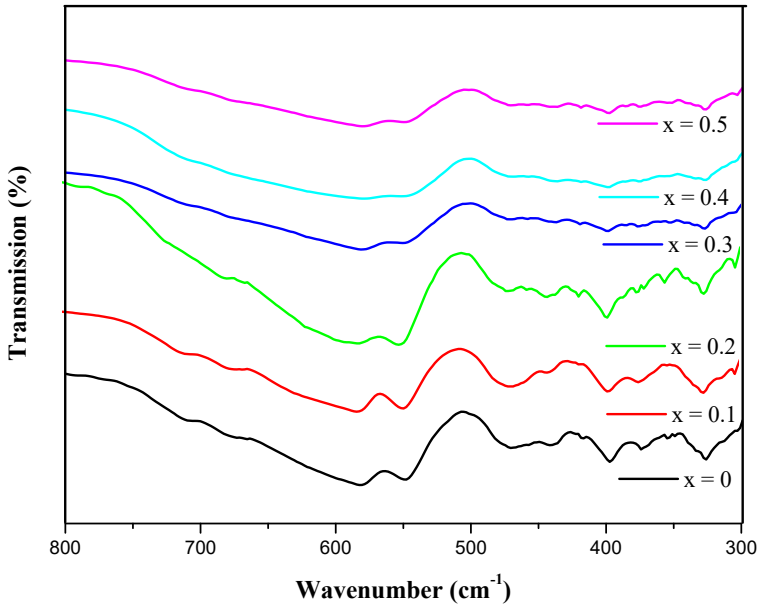

Fig. 4: IRspectra of $Li_{0.5-0.5x}Mg_xFe_{2.5-0.5x}O_4$ ferrites.

The splitting of the absorption bands into several bands has been observed. For all the prepared samplesshow a very clear splitting of the bands. This suggests that the divalent [$Li_{0.5-0.5x}$ $Fe_{2.5-0.5x}$] species in the sample are very well ordered [25]. As concentration of Mg increases the sub bands appears to be smearing and shift to other frequencies.

The observed absorption band corresponding to the tetrahedral complexes ν_1 consists of four sub bands ~710cm^{-1},~ 670cm^{-1}, ~580cm^{-1}, ~548cm^{-1}. This splitting of the main absorption band can be explained by correlating the complex vibrations of the tetrahedral complexes to the octahedral complexes [26]. The splitting of octahedral band into four subbands at ~ 470cm^{-1}, ~395cm^{-1}, ~372cm^{-1} and ~327cm^{-1} is due to the large difference in the reduced mass of the octahedral (Li^+ and Fe^{3+}) complexes.

3.3 Elastic Properties

3.3.1 Force constants:

The force constant per atom was calculated for tetrahedral site (K_t) and octahedral site (K_0) by Waldron method [25], employing the following equations;

$$K_t = 7.62 \times M_A \times \nu_1^2 \times 10^{-7} \text{ N/m} \quad \text{-----(10)}$$

$$K_0 = 10.62 \times \frac{M_B}{2} \times \nu_2^2 \times 10^{-7} \text{ N/m} \quad \text{-------(11)}$$

where M_A and M_B are the molecular weights of cations at A – sites and B-sites, respectively, calculated considering the site occupancies from the suggested cation distribution formula v_1 and v_2 are the wave numbers corresponding to the vibrational frequencies of the cations at the tetrahedral and octahedral sites, respectively.The variation of calculated force constants K_t, K_0 and K_{av} with composition are given in figure (5).

The elastic constants such as Bulk modulus (B), Rigidity modulus (G), Young's modulus (E) and Poisson's ratio (ρ) for all the samples are calculated using IR data and structural data of the present investigation by using following formulae.

Bulk modulus B is given by

$$B = \frac{1}{3}(C_{11} + 2C_{12}) \text{ -----(12)}$$

whereC_{11} and C_{12} are stiffness constants.

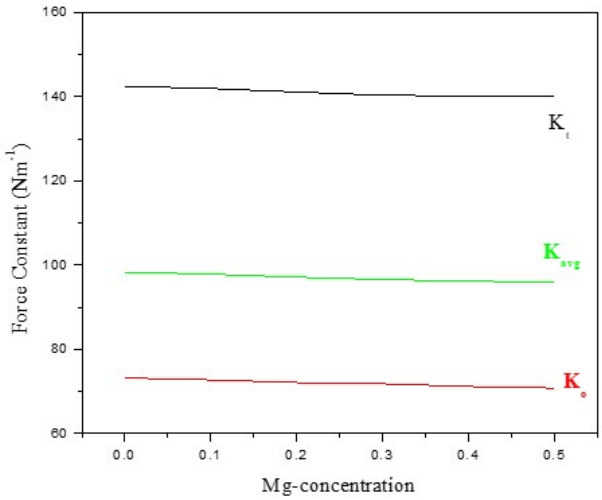

Fig5: Variation force constant K_t, K_o& K_{avg} with Mg-concentration

The bulk modulus is also expressed in terms of the average stiffness constant, hence

$$B = C_{av} \text{ -----(13)}$$

For isotropic materials including spinal ferrites and garnets which have cubic symmetry, stiffness constants are related as: $C_{12} \approx C_{13} \approx C_{44}$ and $C_{11} \approx 3\ C_{44}$[27]. The stiffness constant is also defined as the force constant per lattice constant. Hence, the average stiffness constant can be written as,

$$C_{av} = \frac{k_{av}}{a} \text{ ------(14)}$$

where $k_{av} = \left(\frac{2k_0 + k_t}{3}\right)$ is the average force constant per atom and 'a' is the lattice constant. C_{11} and C_{12} can be written in terms of C_{av} using relations [26]

$$C_{11} = \frac{9C_{av}}{5} \text{ -------(15)}$$

$$C_{12} = \frac{3C_{av}}{5} \text{ ----------(16)}$$

The longitudinal wave velocity (V_l) and transverse wave velocity (V_t) were determined as follows [28]:

$$V_l = \sqrt{\frac{C_{11}}{\rho}} = \sqrt{\frac{9C_{av}}{5\rho}} \text{ -------(17)}$$

$$V_t = \sqrt{\frac{C_{12}}{\rho}} = \sqrt{\frac{3C_{av}}{5\rho}} \text{ --------(18)}$$

The variation of $V_l$withcomposition of Mg-concentration is shown in figure (6). Wave velocities V_l of all the samples found to decrease with Mg concentration.

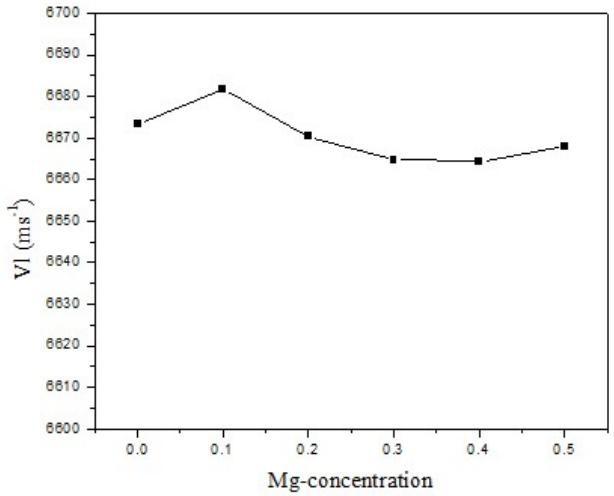

Fig 6: variation of V_l with composition of Mg-concentration.

The other elastic moduli were calculated using the formulae given below [29]:

Rigidity modulus G = ρ x V_t^2 or μ = $\frac{E}{2(1+\rho)}$ -------(19)

Poisson's ratio P = $\frac{(3B-2G)}{(6B+2G)}$ ----------(20)

Young's modulus, E = (1+P) x 2G --------(21)

The obtained values of different elastic moduli are listed in table (3). The elastic moduli B, G and E of all the samples found to decrease with Mg concentration.A plot of the variation of G with respect to E, for each of the samples is given in figure (7), which shows a linear relation. This linear dependence suggests the isotropic elastic nature of these ferrites. From table (3), it was observed that, the poisson's ratio (P) remains constant (∼0.25) for all samples, for isotropic materials it can vary between -1 and +0.5 [30].

Table (3): Elastic moduli B, G and E of $Li_{0.5-0.5x}Mg_xFe_{2.5-0.5x}O_4$ ferrites.

Mg - Concentration	**k_{av}**	**B GPa**	**G GPa**	**P**	**E GPa**
x = 0	98	118.2573	70.95	0.25	177.3859
x = 0.1	98	117.3213	70.39	0.25	175.9819
x = 0.2	97	116.4237	69.85	0.25	174.6355
x = 0.3	97	115.7362	69.44	0.25	173.6042
x = 0.4	96	115.2294	69.14	0.25	172.8442
x = 0.5	96	114.8563	68.91	0.25	172.2845

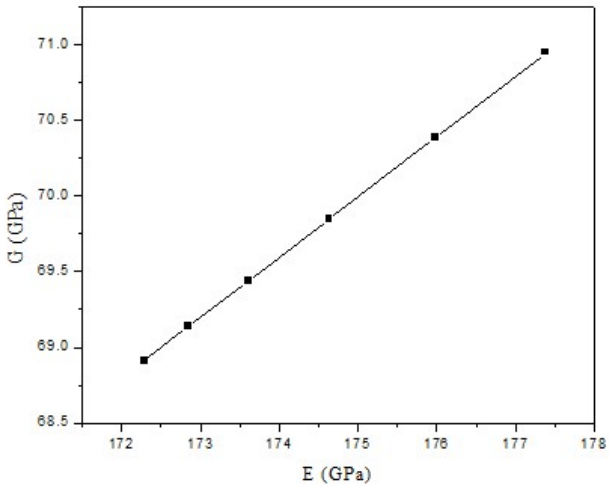

Fig 7: Variation of G with respect to E.

3.4 Debye temperature

The Debye temperature plays an important role in the study of large number of solid-state materials involving lattice vibrations. Physical parameters like elastic constants depend on the Debye temperature of the sample. It provides useful information for thermal properties of the sample.

To calculate the Debye temperature, we adopted two methods viz (Waldronand Anderson).

Debye temperature using the formula suggested by Waldron [25]:

$$\theta_{DW} = \frac{hcv_{av}}{K} \quad \text{-------(22)}$$

where, ν_{av} is the average wave number, h is Planck's constant, k is Boltzmann constant and C is the velocity of light. The calculated θ_{DW} values tabulated in table(4).

Debye temperature using Anderson's formula [31]:

$$\theta_{DA} = \frac{h}{k_B} \text{ x } \left[\frac{3Nq}{4\pi m}\right]^{1/3} \text{ x} V_m \quad \text{--------(23)}$$

where, h is Planck's constant, k_B Boltzmann constant, N Avogadro number, M molecular weight of the sample, q is the number of atoms in a moleculeand velocity as defined below;

Table (4): The values of V_l, V_t, V_m θ_{DW} and θ_{DA}

Mg - Concentration	B=C_{av} GPa	ρ_{xray}	$V_{l\text{-xray}}$ m/s	$V_{t\text{-xray}}$ m/s	$V_{m\text{-xray}}$ m/s	Debye Temperature Waldron K	Debye Temperature Anderson K
x = 0	116.64	4.78	6627.51	3826.39	4248.02	704.37	582.07
x = 0.1	116.33	4.73	6653.65	3841.49	4264.78	705.81	583.26
x = 0.2	115.09	4.71	6632.11	3829.05	4250.97	705.81	580.56

x = 0.3	113.86	4.69	6610.74	3816.71	4237.27	705.81	578.80
x = 0.4	113.82	4.67	6623.69	3824.19	4245.57	704.37	580.06
x = 0.5	112.58	4.65	6601.71	3811.49	4231.48	704.37	577.30

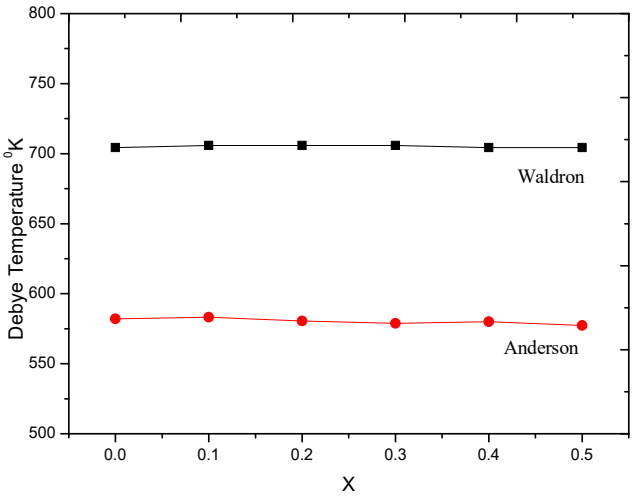

Fig 8: Debye temperature using Anderson and Waldron models with Mg-concentration.

$$V_m = \frac{1}{3} x \left(\frac{2}{V_t^3} + \frac{1}{V_l^3}\right)^{-1/3} \quad \text{-------(24)}$$

The values of V_m are tabulated in table (4). The plot of Debye temperature using both methods versus Mg-concentration shown in figure (8), both these values show good agreement with each other. The Debye temperature calculated using the Waldron method ($\theta_{DW} \approx$ 705 K) is higher than that calculated using Anderson's equation ($\theta_{DA} \sim$ 580 K).

4. **Conclusions:**All the major peaks of $Li_{0.5-0.5x}Mg_xFe_{2.5-0.5x}O_4$ prepared samples are indexed using 'POWDER X' software confirming the formation of cubic spinel ferrite. The substitution of Mg^{2+} ions in Lithium ferrites obeying Vegard's law. Cation distribution is suggested based on the X-ray data and its validity is done by the calculation of lattice parameters a_{th} and $a_{exp}$and are in close agreement. IR spectra of all prepared spinel ferrites confirms the substitution of Mg^{2+} are occupying octahedral and tetrahedral sites of spinel ferrites. The linear dependence of rigidity modulus with young's modulus suggests the isotropic nature of spinel ferrites. Debye temperature of all prepared ferrites are calculated using Waldron and Anderson model and are in agreement with reported values.

References

1. G. O. White and C. E. Patton, J. Magn. Magn. Mater. 9 (1978) 299.
2. G. M. Argentina and I. D. Baba, IEEE Trans. Microwave Theory Techn. 22 (1974) 654.
3. N. Gupta, S. C. Kashyap and D. C. Dube, J. Magn. Magn. Mater. 288 (2005) 307.

4. X. M. Liu, S. Y. Fu, H. M. Xiao and C. J. Huang, Physica B: Condens. Mater. 370 (2005) 14.
5. C. Sun and K. Sun, J. Physica B 391 (2007) 335.
6. B. K. Nath, P. K. Chakrabari, S. Das, U. Kumar, P. K. Mukhopadhyay and D. Das, European Physical Journal B: Condens. Mater. & Comp. System. 39 (2004) 417.
7. H. M. Sung, C. J. Chen, W. S. Ko and H. C. Lin, IEEE Trans. Magn. 30 (1994) 4906.
8. U. Hafeli, W. Schutt, J. Teller and M. Zborowski (Eds.), (Plenum Press), NY, USA, 1997.
9. Z. Yue, J. Zhou, X. Wang, Z. Gui and L. J. Li, J. Mater. Sci. Lett. 20 (2001) 1327.
10. W. C. Kim, S. J. Kim, S. W. Lee and C. S. Kim, J. Magn. Magn. Mater. 226-230 (2001) 1418.
11. Qi Chen, A. J. Rondinone, B. C. Chakoumakos and Z. J. Zhang, J. Magn. Magn. Mater. 194 (1999) 1.
12. T. Sasaki, S. Ohara, T. Naka, J. Vejpravova, U. Sechovsky, M. Umetsur, S. Takami, B. Jeyadevan and T. Adschiri, J. Supercrit. Fluids 53 (2010) 92.
13. E. J. Choi, Y. Ahn, S. Kim, D. H. An, K. U. Kang, B. G. Lee, K. S. Beak and H. N. Oak, J. Magn. Magn. Mater. 262 (2003) L198.
14. A. Pradeep, C. Thangasamyand G. Chandrasekaran, J. Mater. Sci: Mater. Electron 15 (2004) 797.
15. S. Lature, S. Kalashetty and G. H. Jadhav, Phys, Scr. 90 (2015) 085805.
16. J. S. Baijal, S. P. Joubam, D. Kothari, C. Prakash and P. Kishan, Solid Stat. Commun. 83 (1992) 679.
17. H. M. Widatallah, C. Johson, F. Berry and M. Pekala, Solid Stat. Commun. 120 (2001) 171.
18. Y. Purushottam, M. B. Reddy, P. Kishan, D. R. Sagar and P. V. Reddy, Mater. Lett. 17 (1993) 341.
19. B. P. Bhandare, R. M. Sangshetty, S. Lature and G. H. Jadhav, Int. Res. J. Sci. & Engg., A5 (2018) 69.
20. Y. P. Fu and S. H. Hu, Ceramics Int., 36 (2010) 1311.
21. K. J. Standley, Oxide Magn. Mater., (London: Clarendon Press).
22. S. A. Mazen, A. E. Abd El-Rahiem and B. A. Sabrah, J. Magn. Sci. 23 (1988) 2917.
23. S. A. Mazen, M. H. Abdallah, R. I. Nakhla, F. Metawe and H. M. Zaki, Mater. Chem. Phys. 34 (1993) 35.
24. S. C. Watawe, B. D. Sutar, B. D. Sarwade and B. K. Chougule, J. Inorg. Mater. 3 (2001) 819.
25. R. D. Waldron, Phys. Rev. 99 (1955) 1727.
26. V. Rathod, Anupama A. V, R. Vijaykumar, V. M. Jali and B. Sahoo, Vibrational Spectroscopy 92 (2017) 267.
27. S. L. Kakani and C. A. Hemrajani, Text Book of Solid State Physics, Third Ed., Sultan Chand & Sons, New Delhi (1997) 150.
28. W. A. Wooster, Rep. Prog. Phys. 16 (1953) 62.
29. B. Raj, V. Rajendram and P. Palanichamy, Science & Technology of Ultrasonics, Narosa Pub. House, New Delhi, (2004) 250.
30. N. I. Abu-Elsaad, J. Mole. Stru., 1075 (2014) 546.
31. O. L. Anderson, Physical Acoustics III B, Academic Press, New York (1965) 43.